Large Area Avalanche Photo Diodes (LAAPD)

LAAPD are very useful as alternative photo-detector.

Advantage the APD in comparison PMT is:

- not sensitivity to magnetic field of (up to 7.9 Tesla was measurement);
- high quantum efficiency from deep UV (150nm) to IR spectra;
- small rate effect;
- high linearity;
- high response uniformity;
- highly radio-pure;
- smaller size…

Disadvantage is:

- size of active area;
- temperature sensitivity of gain and noise;
- excess noise factor;
- electronic noise (limitation of gain imply to use the preamplifier)

Also APD is very fast and effective detector for charge particles.

In this paper submit large area APD (>20mm²) produced by:

- Hamamatsu Inc. - 5x5mm² and 10x10mm²;
- Advanced Photonics Inc. – D5, D10 and D16 mm;
- Radiation Monitoring Devices Inc. – 8x8mm², 13x13mm².

Most important characteristics of APD is size of active area, quantum efficiency, capacitance, dark current, excess noise factor, rise time, serial resistance, maximum of gain…

Energy resolution of APD

Energy resolution of APD:

$\sigma^2_E = (\sigma^2_{stat} + \sigma^2_{noise})/N_{ph}$, were σ_{stat} – statistical contribution in photoelectrons, σ_{noise} - APD noise contribution in photoelectrons

$\sigma^2_{stat} = F/N_{ph.el}$, were F -excess noise factor, $N_{ph.el}$ – number of photoelectrons

- $N_{ph.el} = N_{ph} * Q$, were N_{ph} – number of primary photons, Q - quantum efficiency of APD
- $F = k_{eff} M + (1-k_{eff})(2-1/M)$, were k_{eff} - ratio of the hole and electron ionization rates, M –gain of APD

Noise contribution of APD

$\sigma^2_{noise} = \sigma^2_{dc} + \sigma^2_{elec.} \sim (I_{ds}/M^2 + I_{db}F)\Delta t/q + 4kT[R_S(C_{det}/C_{tot})^2 + 1/g_m]C^2_{tot}/q^2M^2\tau$, were σ^2_{dc} – dark current (parallel) noise in photoelectrons , $\sigma^2_{elec.}$ – electronic (serial) noise in photoelectrons

- $\sigma^2_{dc} = \sigma^2_{ds} + \sigma^2_{db} \sim (I_{ds}/M^2 + FI_{db})\Delta t/q$, were σ_{ds} – noise of surface current, σ_{db} – noise of bulk current, I_{ds} – surface current, I_{db} – bulk current, q- electron charge, Δt - integrating time interval

$I_{dc} = I_{ds} + I_{bc}M$

- $\sigma^2_{elec.} \sim 4kTR_SC^2_{tot}/q^2M^2\tau = N^2_{p/ampl}/M^2$, were R_S -serial resistance of APD, k -Boltzman constant, T- temperature

$C_{tot} = C_{det} + C_{p/amp}$, were C_{det} - capacitance of APD, $C_{p/amp}$ - input capacitance of preamplifier

The correct measurement of gain is very important for characterized APD. The gain of APD sensitive to temperature and all measurements need make in same conditions.

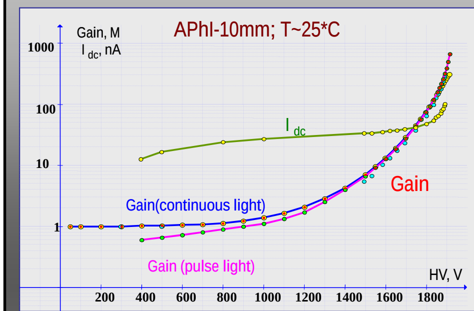

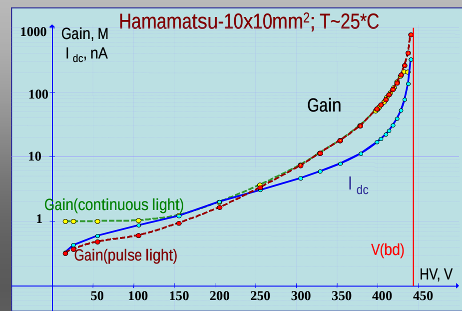

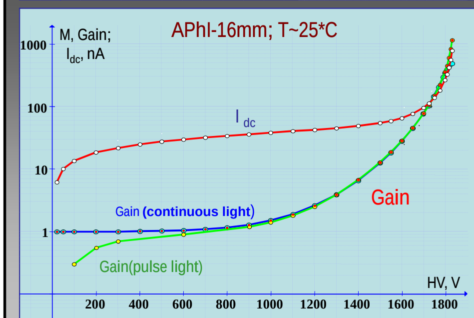

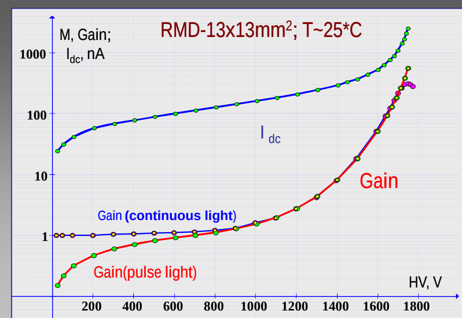

With continuous light easy make accurately measurement the gain in region until ~10-s without changing intensity of illumination, because in this case (DC) photocurrent not depends capacitance of APD in contrast to pulse measurement.

$M(V) = [I_{light+DC}(V) - I_{DC}(V)] / I_{light}(100V)$

For range of gain from 10s to 1000 more useful pulse light measurement (without changing intensity of illumination), because in this region of HV the capacitance of APD almost constant and have not current limitation in contrast to continuous light measurement.

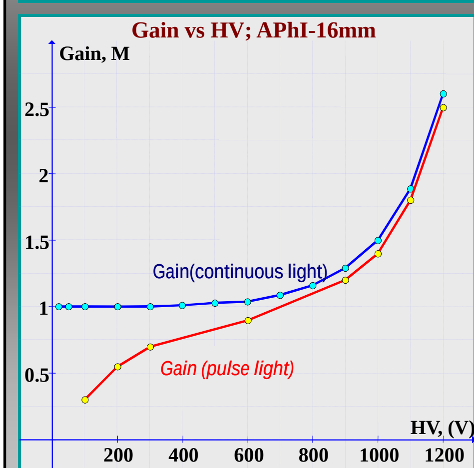

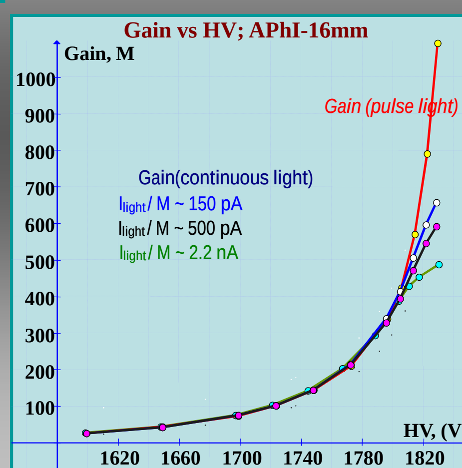

Using DC measurements of leakage current (I_{dc} vs HV) and the gain (M vs HV) we can find out value of the surface and bulk currents. $I_{dc} \sim I_{sc} + I_{bc} * M$.

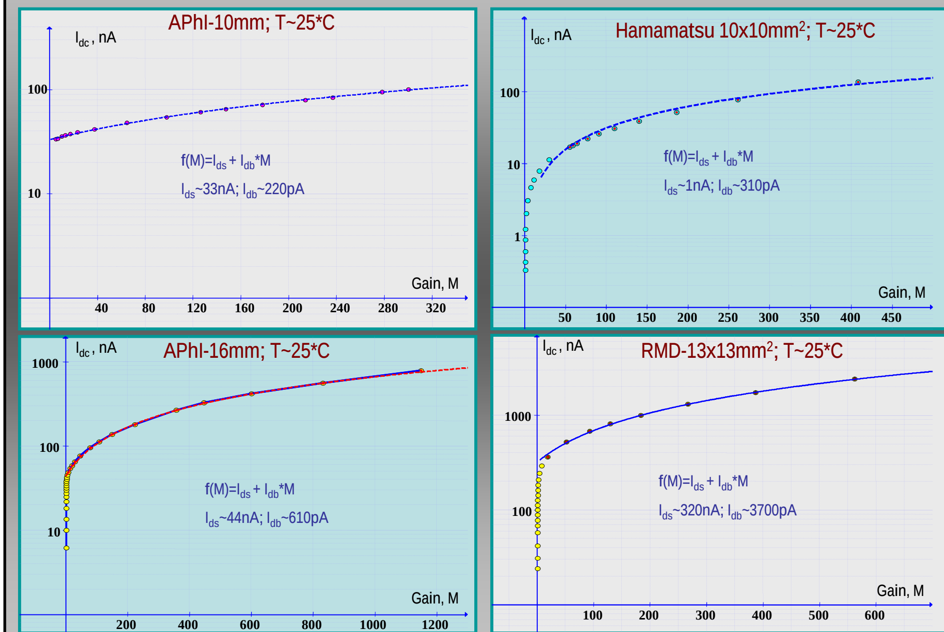

Using fast pulse of light (blue LED) we can measure rise and fall time of APD (no preamplifier).

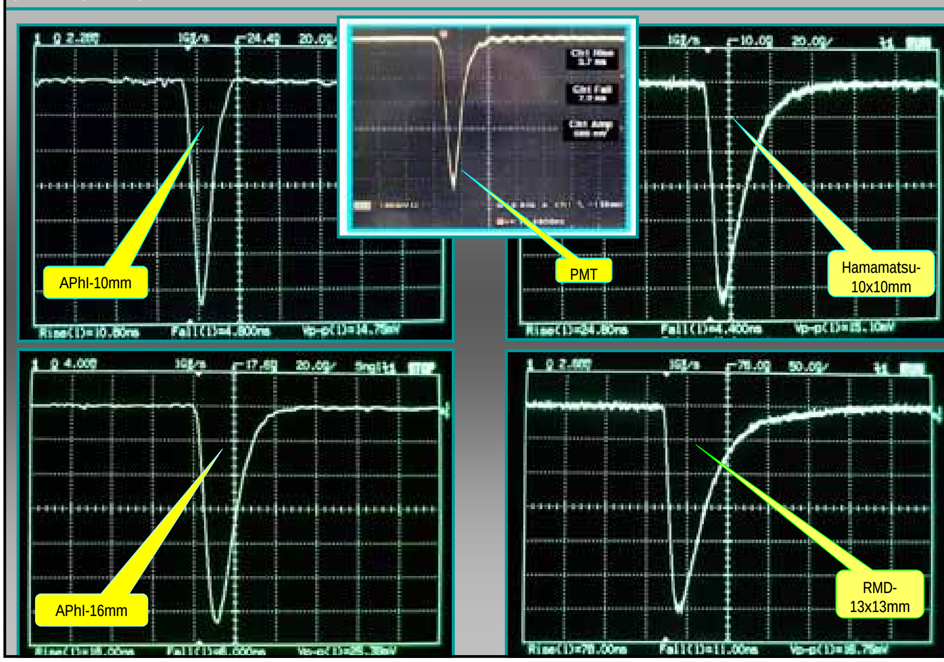

Using value of capacitance of APD and measured fall time we can find out the serial resistance of APD.

$R_S = \tau_r / C_{det} - 50\ \Omega$

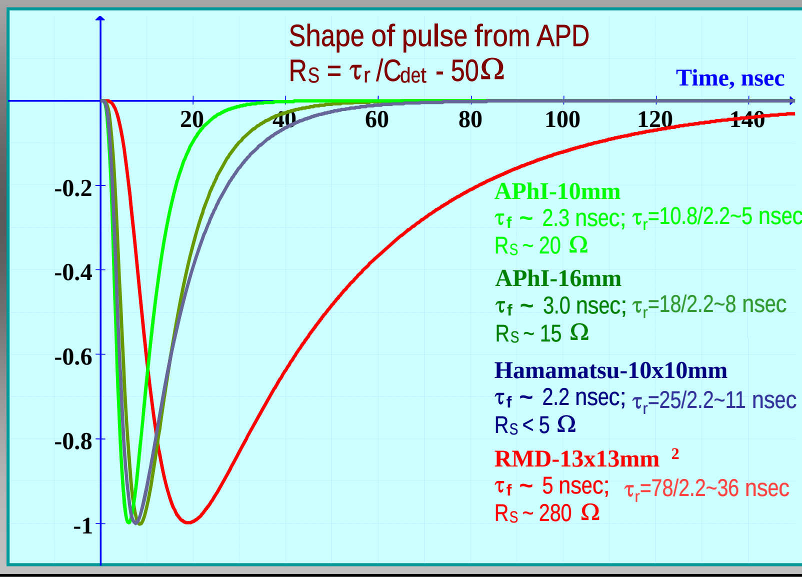

The excess noise factor depends internal structure of APD, profile of the electric field and gain. We can measure the excess noise factor of APD by measuring σ_{light} of same light and σ_{PED} vs gain.

$N(M)=1/(\sigma^2_{light} - \sigma^2_{PED})= N_{ph.el.}/F$, were $F \sim k_{eff}M+(1-k_{eff})(2-1/M)$

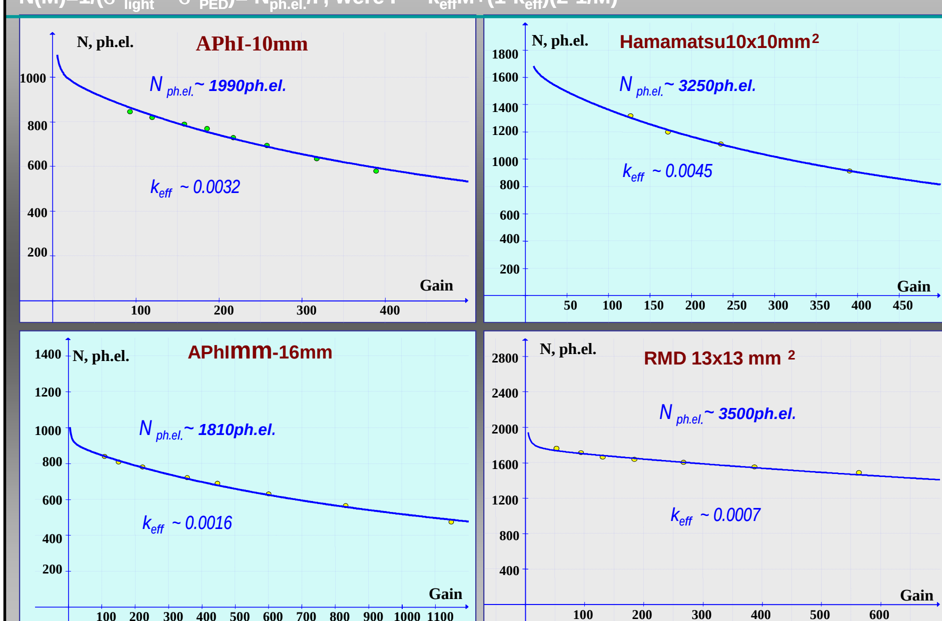

Using PED measured and scale factor ch-ph.el we can find out the bulk current I_{bc} **(a)**, the excess noise factor k_{eff} **(b)** and noise of electronics (APD-p/amp chain) $N_{elec.noise}$ **(c)** of APD.

σ_{PED} = sqrt(a*(b*M+(1-b)(2-1/M)) + c^2/M^2) were $a=qI_{bc}\Delta t$, $b=k_{eff}$ and $c=N_{elec.noise}$ (T~25*C)

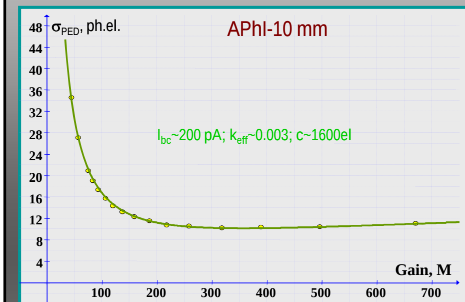

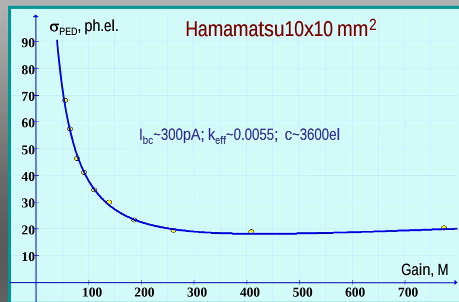

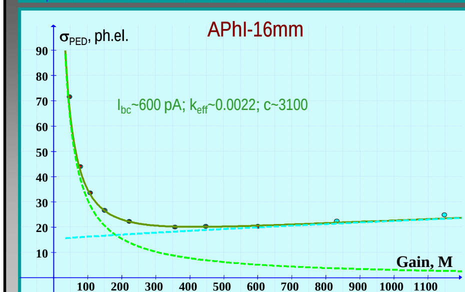

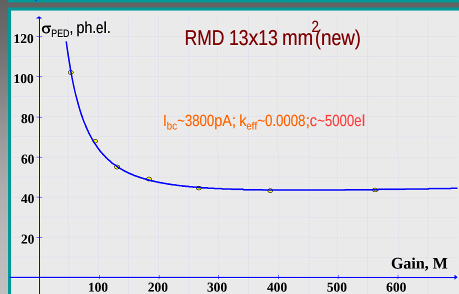

Choice of shaping time and gain

- Charge sensitive p/amplifier making better signal-noise ratio, but increasing pile-up effect.
- Shorter shaping time reducing the noise of dark current and reducing pile-up effect, but increasing the noise of preamplifier. That noise can be reducing by higher gain, but higher gain increasing excess noise factor which will affect the statistical accuracy of signal.
- For different scintillator need optimize shaping time and gain for full integration of the light pulse and have better statistical accuracy and have less noise for better signal-noise ratio.
- For light from organic scintillator (or crystal with short decay time τ_d<10nsec) and for APhI-16mm and APhI-10mm the optimum of shaping time ~20nsec, for RMD-13x13mm^2 ~ 30nsec.

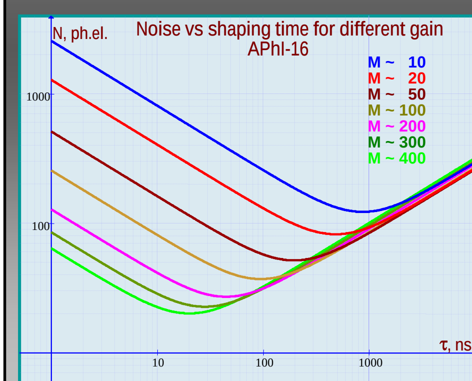

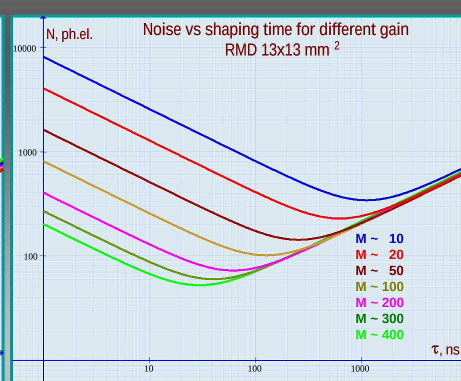

For module EM Calorimeter "SHASHLYK" we proposed charge sensitive preamplifier with shaper (shaping time ~20nsec), because decay time of light from module ~ 8nsec and choused gain of APD M~200-300.

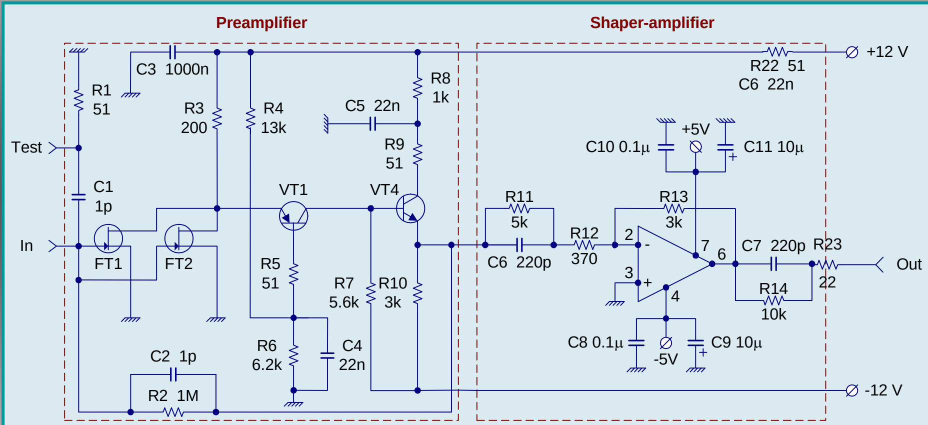

J1 and J2 are the Russian 2P341A JFETs (analog is 2SK394-5 YJ5 JFET, SANYO).
VT1 - VT3 are the Russian 2T363A bipolar transistors (analog is 2N4260).
VT4 - VT6 are the Russian 2T368A bipolar transistors (analog is 2N3600).
All schematic components are the surface-mount elements.

Measured noise of APD with charge sensitive preamplifier (shaping time ~20nsec) vs gain for different temperature.

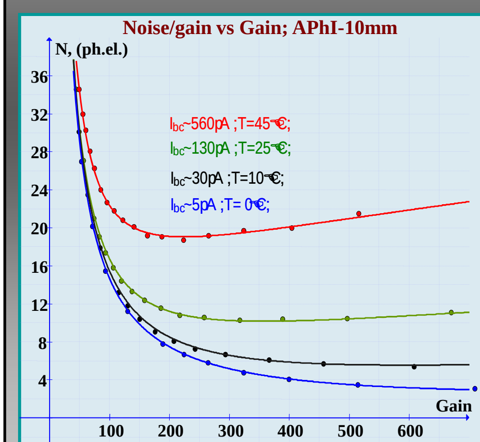

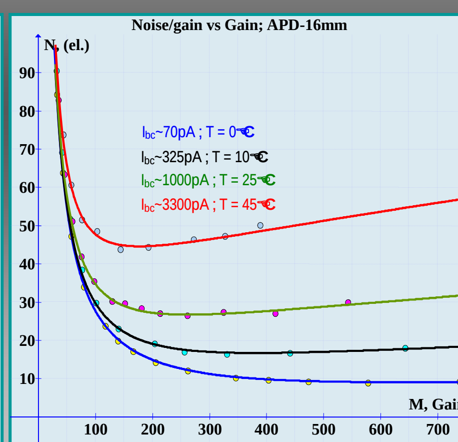

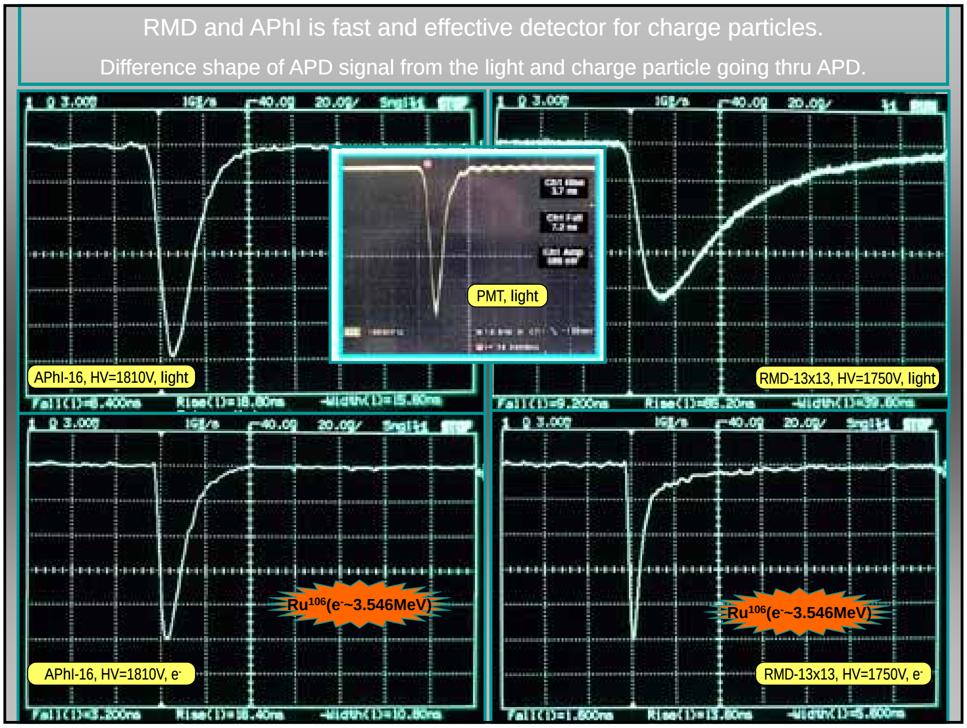
RMD and APhI is fast and effective detector for charge particles.
Difference shape of APD signal from the light and charge particle going thru APD.
APhI-16, HV=1810V, light
PMT, light
RMD-13x13, HV=1750V, light
Ru106(e-~3.546MeV)
APhI-16, HV=1810V, e-
Ru106(e-~3.546MeV)
RMD-13x13, HV=1750V, e-

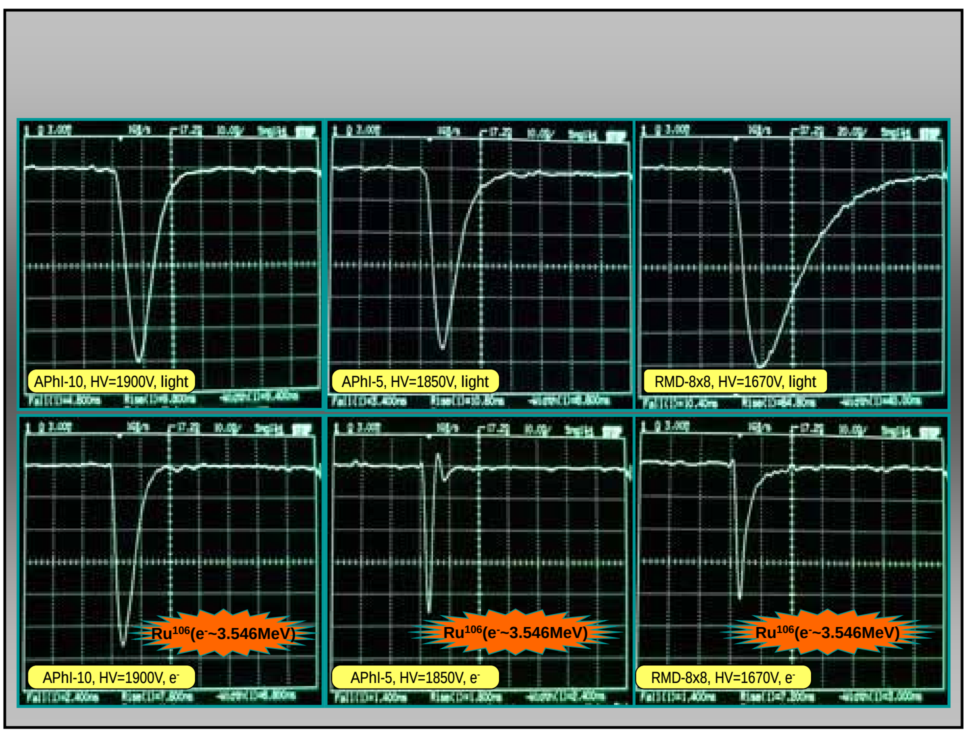
APhI-10, HV=1900V, light
APhI-5, HV=1850V, light
RMD-8x8, HV=1670V, light
Ru106(e-~3.546MeV)
APhI-10, HV=1900V, e-
Ru106(e-~3.546MeV)
APhI-5, HV=1850V, e-
Ru106(e-~3.546MeV)
RMD-8x8, HV=1670V, e-

Temperature sensitivity (**1/M dM/dT) and** HV sensitivity (**1/M dM/dV) vs gain for different temperature.**

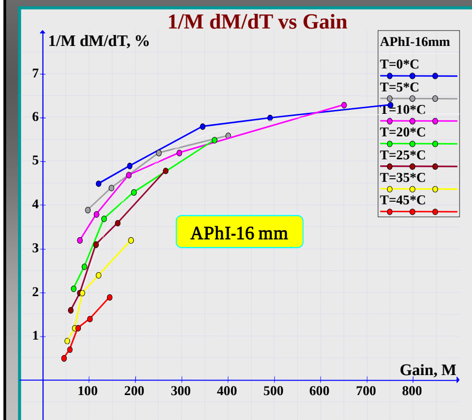

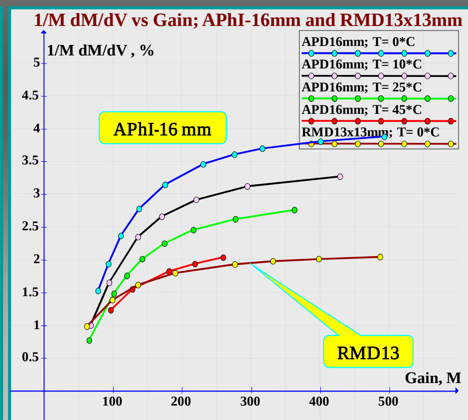

T~25°C		APhI-D16	APhI-D10	APhI-D5	RMD 8x8	RMD 13x13	S8664-55 S8148(CMS)	S8664-1010N	EG&G C30703
Active area (mm^2)		~200	~80	~20	~64	~170	~25	~100	~100
Q.E.	~400nm ~650nm	~80 ~90	~80 ~90	~80 ~90	~60 ~70	~60 ~70	~75 ~80	~75 ~80	~70 ~80
Capacitance (pF)		~130	~65	~25	~60	~110	~90	~270	~80
R_S (Ω)		~15	~15	~10	~400	~50(~280)	<5	<5	~10
Fall time (ns)	Light ch.partic.	~6 ~3.2	~4.8 ~2.4	~4 ~1.5	~7 ~1.4	~10 ~1.6	~2 ?	~4.4 ?	~5 ?
Rice time (ns)	Light ch.partic.	~16 ~16	~9 ~8	~8 ~1.6	~60 ~10+	~24(~80) ~14+	~16 ?	~25 ?	~15 ?
k_{eff}		~0.002	~0.003	~0.003	~0.0008	~0.0008	~0.006	~0.005	~0.02
Gain, M		<600	<600	<600	<1000	<1000	<300	<300	<200
I_{ds} , nA		~50	~30	~25	~120	~300	~1	~1	~10
I_{db} , nA		~0.61	~0.22	~0.1	~1.1	~3.7	~0.15	~0.31	~0.4
1/M dM/dT, % (M~200)		~4	~4	~4	~4	~4	~6	~6	~6
1/M dM/dV, % (M~200)		~2.5	~2.5	~2.5	~1.8	~1.8	~5	~5	~5
$\sigma_{elec.\ noise}$, *[el]*		~3100/M	~1600/M	~900/M	~3500/M	~5000/M	~2000/M	~3600/M	~1200/M
σ_{ds}, *[el]*		~100/M	~80/M	~70/M	~180/M	~280/M	~15/M	~15/M	`~40/M
σ_{db}, *[el]*		~11*$F^{1/2}$	~6.5*$F^{1/2}$	~4.5*$F^{1/2}$	~15*$F^{1/2}$	~28*$F^{1/2}$	~5.5*$F^{1/2}$	~8*$F^{1/2}$	~7*$F^{1/2}$
F(M=200)		~2.4	~2.5	~2.5	~2.16	~2.16	~3.2	~3	~4
σ_{noise},*(M=200), [el]*		~23	~13	~8.5	~28	~48	~14	~23	~15

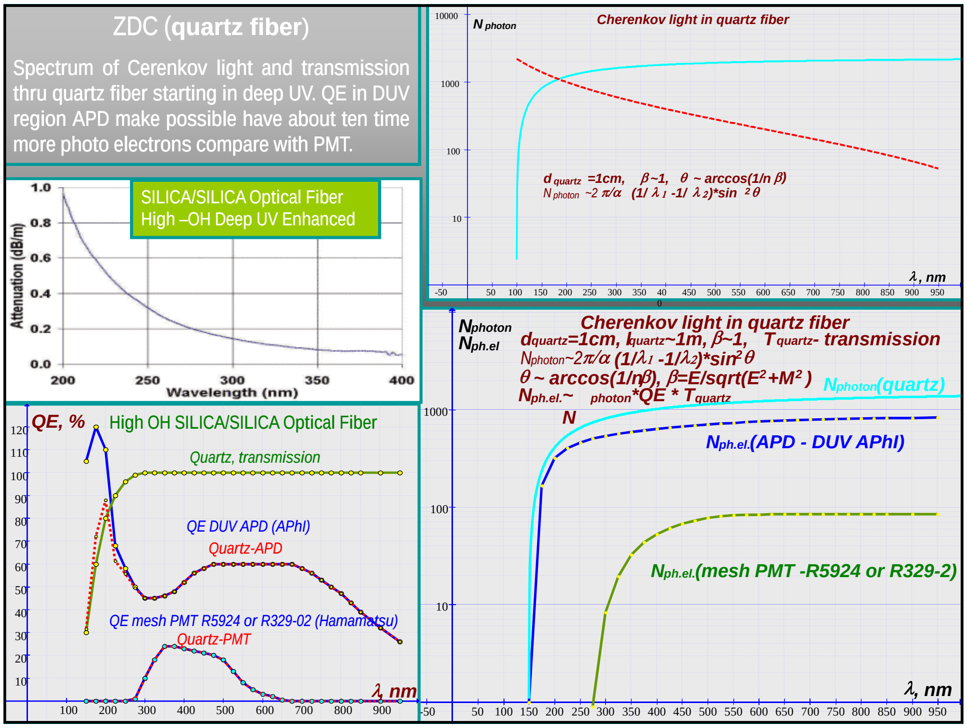
ZDC (quartz fiber)
Spectrum of Cerenkov light and transmission thru quartz fiber starting in deep UV. QE in DUV region APD make possible have about ten time more photo electrons compare with PMT.
SILICA/SILICA Optical Fiber High –OH Deep UV Enhanced
Attenuation (dB/m)
Wavelength (nm)
Cherenkov light in quartz fiber
N photon
λ, nm
QE, %
High OH SILICA/SILICA Optical Fiber
Quartz, transmission
QE DUV APD (APhI)
Quartz-APD
QE mesh PMT R5924 or R329-02 (Hamamatsu)
Quartz-PMT
λ, nm
Nphoton
Nph.el
Cherenkov light in quartz fiber
Nphoton(quartz)
Nph.el.(APD - DUV APhI)
Nph.el.(mesh PMT -R5924 or R329-2)
λ, nm

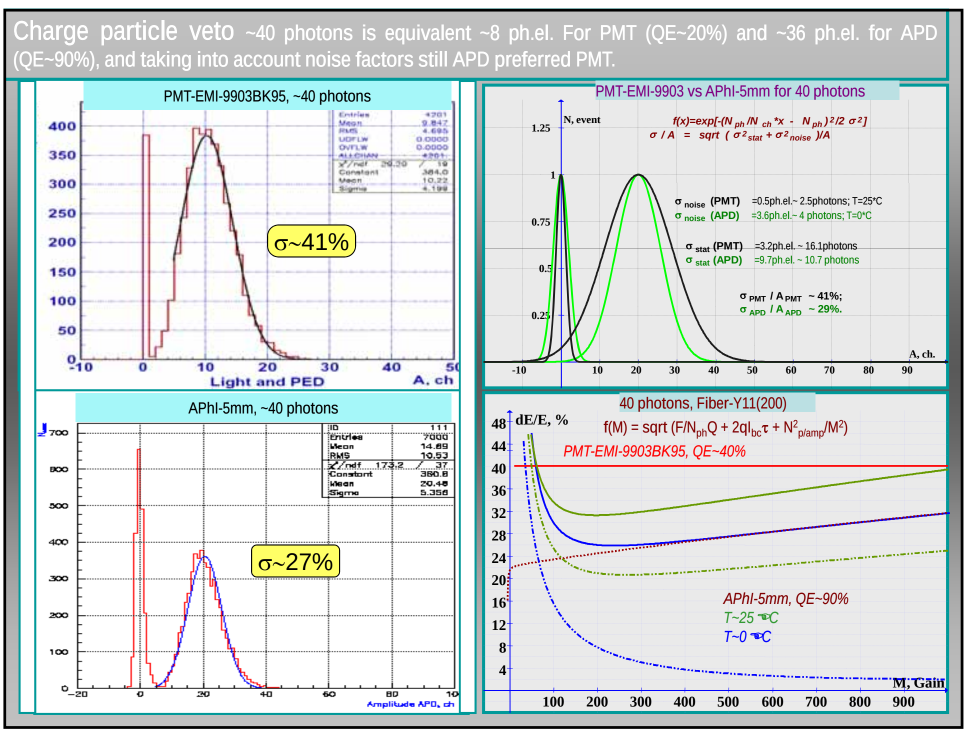
Charge particle veto ~40 photons is equivalent ~8 ph.el. For PMT (QE~20%) and ~36 ph.el. for APD (QE~90%), and taking into account noise factors still APD preferred PMT.
PMT-EMI-9903BK95, ~40 photons
σ~41%
Light and PED
A, ch
APhI-5mm, ~40 photons
σ~27%
Amplitude APD, ch
PMT-EMI-9903 vs APhI-5mm for 40 photons
N, event
A, ch.
σ PMT / A PMT ~ 41%;
σ APD / A APD ~ 29%.
40 photons, Fiber-Y11(200)
dE/E, %
PMT-EMI-9903BK95, QE~40%
APhI-5mm, QE~90%
T~25 °C
T~0 °C
M, Gain

Liquid Xenon, Liquid Argon and Liquid Neon in the future (R&D ongoing at Yale), most promising and cost-effective materials for detection WIMP in Dark Matter experiments.

- low light (tens photons);
- deep ultra violet spectrum (~170nm);
- low temperature (~ 50-180K);
- highly radio-purity…

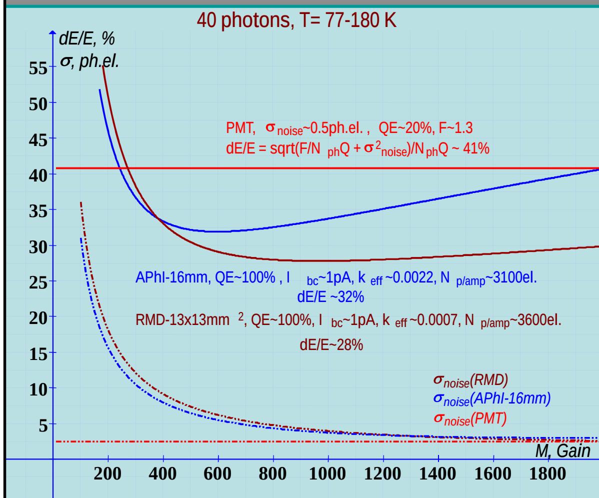

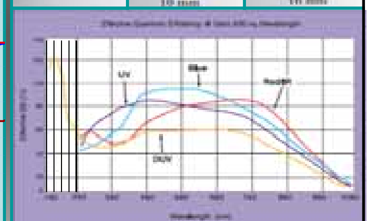

Radio isotopes in PMT

U-chain (Bq)	Th-chain (Bq)	^{40}K (Bq)	^{60}Co (Bq)
1.8×10^{-2}	6.9×10^{-3}	1.4×10^{-1}	5.5×10^{-3}

We saw same reducing dark current after switch on HV. These effects we saw for all type APD.

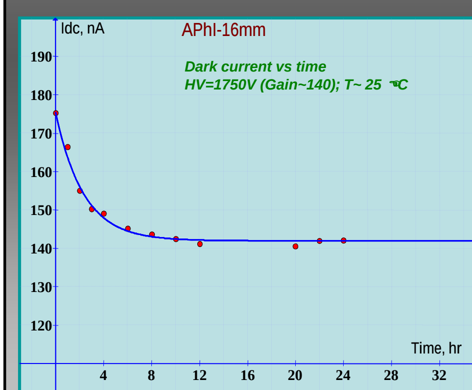

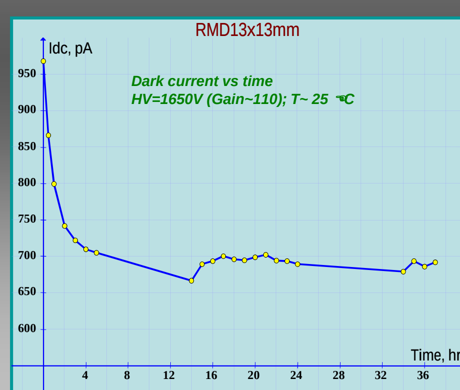

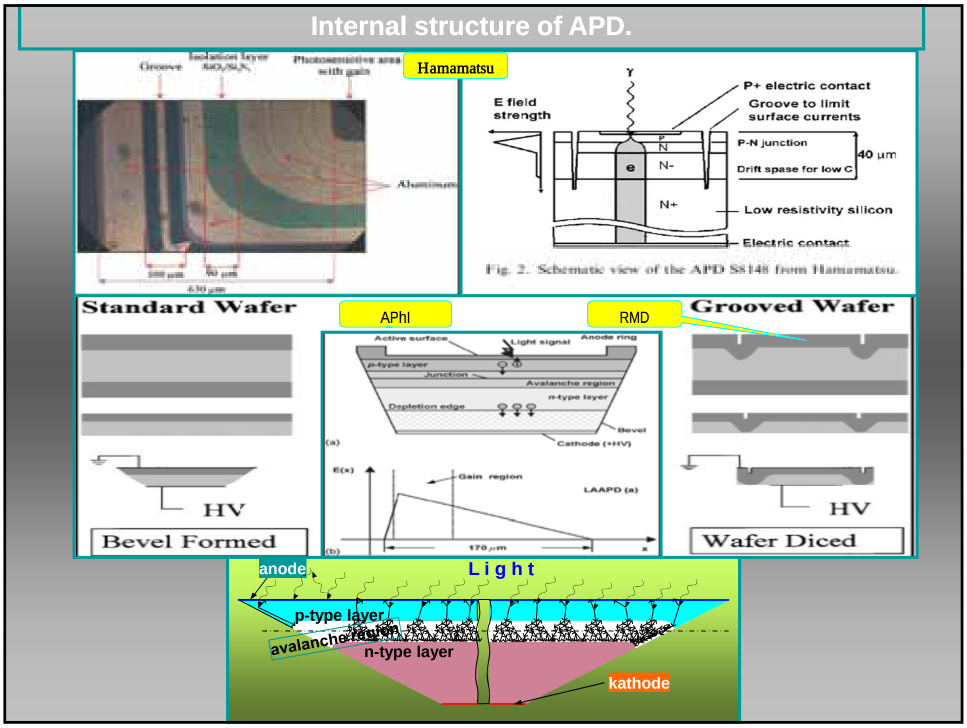

Internal structure of APD.
Hamamatsu
Groove
Isolation layer
Photosensitive area with gain
Aluminum
E field strength
P+ electric contact
Groove to limit surface currents
P-N junction
40 µm
Drift spase for low C
N-
N+
Low resistivity silicon
Electric contact
Fig. 2. Schematic view of the APD S8148 from Hamamatsu.
Standard Wafer
APhI
RMD
Grooved Wafer
Active surface
Light signal
Anode ring
p-type layer
Junction
Avalanche region
n-type layer
Depletion edge
Bevel
Cathode (+HV)
E(x)
Gain region
LAAPD (a)
170 µm
HV
Bevel Formed
Wafer Diced
anode
Light
p-type layer
avalanche region
n-type layer
kathode